Rupestines F—M, New Guaipyridine Sesquiterpene Alkaloids from *Artemisia rupestris*

Fei He,[a,b] Alfarius Eko Nugroho,[a] Chin Piow Wong,[a] Yusuke Hirasawa,[a] Osamu Shirota,[c] Hiroshi Morita,*,[a] and Haji Akber Aisa*,[b]

[a] *Faculty of Pharmaceutical Sciences, Hoshi University; 2–4–41 Ebara, Shinagawa-ku, Tokyo 142–8501, Japan:* [b] *Key Laboratory of Chemistry of Plant Resources in Arid Regions, Xinjiang Technical Institute of Physics and Chemistry, Chinese Academy of Sciences; Beijing South Road 40–1, Urumqi, Xinjiang 830011, P.R. China: and* [c] *Faculty of Pharmaceutical Sciences at Kagawa Campus, Tokushima Bunri University; 1314–1 Shido, Sanuki, Kagawa 769–2193, Japan.* Received October 19, 2011; accepted November 25, 2011; published online December 2, 2011

Eight new guaipyridine sesquiterpene alkaloids, rupestines F—M (1—8) were isolated from the leaves of *Artemisia rupestris* and their structures were elucidated on the basis of 2D-NMR data. The absolute configurations of 1—8 have been assigned by comparison of their experimental and calculated circular dichroism (CD) spectra.

Key words *Artemisia rupestris*; rupestine; guaipyridine sesquiterpene alkaloid; circular dichroism; absolute configuration

Artemisia rupestris L. (Compositae) is a well-known traditional Chinese medicinal plant in Xinjiang Province of China used for detoxification, antitumor, antibacterial, antivirus, and protecting liver.[1,2] It is also a well-known rich source of unique sesquiterpenes such as rupestonic acid showing anti-virus activity.[3] Recently, five new sesquiterpene alkaloids, which have attracted great attention in the biogenetic and biological points of view, have been isolated from the flower of this plant.[4,5] In our further efforts to search for the structurally interesting metabolites from *A. rupestris*, eight new guaipyridine sesquiterpene alkaloids, rupestines F—M (**1**—**8**) were isolated from the leaves. We applied density functional theory (DFT) calculations for determination of absolute configuration (AC) of **1**—**8**, after conformational analysis of them. In this paper, we described the isolation and structure elucidation including ACs of **1**—**8** with pyridine cycloheptene ring system (Chart 1).

The alkaloid fraction prepared from acid-base solvent partitions of the methanol extract from the leaves of *A. rupestris* was separated using silica gel column, Sephadex LH-20 column, amino silica gel column, and preparative HPLC to give eight sesquiterpene alkaloids, rupestines F—M (**1**—**8**).

Rupestine F (**1**) had molecular formula of $C_{16}H_{21}NO_2$ determined by high resolution-electrospray ionization-mass spectrometry (HR-ESI-MS) [*m/z* 260.1671 $(M+H)^+$]. The UV absorption maxima at 270 nm was characteristic of a typical alkyl-substituted pyridine.[6] IR absorptions suggested the presence of a carbonyl (1723 cm^{-1}) and a pyridine unit (1591, 1461 cm^{-1}). The ^{1}H-NMR spectrum (Table 1) revealed a typical AB pattern for the protons at δ_H 6.93 (d, 7.6) and δ_H 7.31 (d, 7.6), one methyl group attached to the pyridine nucleus resonated at δ_H 2.48,[7] one methoxy at δ_H 3.76, and two singlet signals at δ_H 5.61 and 6.19 belonging to exo-methylene protons. ^{13}C-NMR data (Table 2) revealed 16 carbon signals due to one carbonyl, four sp^2 quaternary carbons, two sp^2 methines, one sp^2 methylene, two sp^3 methines, three sp^3 methylenes, and three methyls.

Partial structures of C-5 to C-9 and C-16 were deduced from analysis of ^{1}H–^{1}H correlation spectroscopy (COSY) and heteronuclear multiple bond connectivity (HMBC) spectra (Fig. 1). The HMBC correlations of H_3-15 to C-2 and C-3, H-3 to C-11, and H-4 to C-10 showed that the existence of a tri-substituted pyridine ring (Fig. 1). The HMBC cross-peaks of H_3-16 and H_2-9 to C-11, and H_2-9 to C-10 confirmed that a

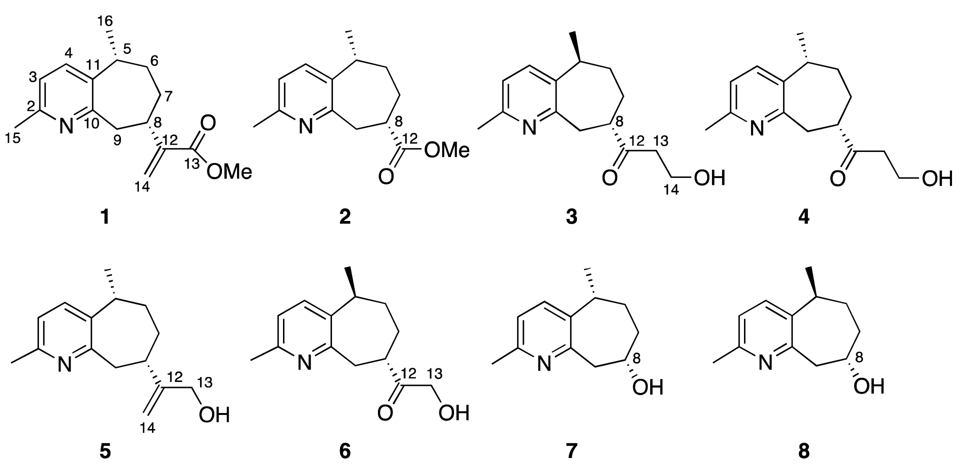

Chart 1

* To whom correspondence should be addressed. e-mail: moritah@hoshi.ac.jp; haji@ms.xjb.ac.cn

Table 1. ^{1}H-NMR Data [δ_H (J, Hz)] of Rupestines F—M (**1**—**8**) in $CDCl_3$

	1	**2**	**3**	**4**	**5**	**6**	**7**	**8**
3	6.93 (d, 7.6)	6.93 (d, 7.9)	6.99 (d, 7.9)	6.97 (d, 8.0)	6.95 (d, 7.6)	7.02 (d, 8.0)	6.97 (d, 8.0)	6.97 (d, 8.0)
4	7.31 (d, 7.6)	7.30 (d, 7.9)	7.43 (d, 7.9)	7.36 (d, 8.0)	7.34 (d, 7.6)	7.41 (d, 8.0)	7.35 (d, 8.0)	7.37 (d, 8.0)
5	3.05 (m)	2.99 (m)	2.98 (m)	3.01 (m)	3.07 (m)	3.02 (m)	2.96 (m)	2.96 (m)
6α	1.82 (2H, m)	2.01 (m)	1.91 (m)	1.79 (2H, m)	1.82 (m)	1.97 (m)	1.67 (2H, m)	1.86 (m)
6β		1.76 (m)	1.25 (m)		1.72 (m)	1.31 (m)		1.34 (m)
7α	1.83 (2H, m)	1.95 (m)	1.86 (m)	1.83 (m)	1.83 (2H, m)	1.97 (m)	1.95 (m)	1.87 (m)
7β		2.12 (m)	2.05 (m)	2.02 (m)		2.03 (m)	2.05 (m)	2.18 (m)
8	2.83 (m)	2.64 (m)	2.58 (m)	2.80 (m)	2.42 (m)	2.58 (m)	4.13 (m)	3.78 (m)
9α	3.24 (dd, 14.4, 10.0)	3.36 (dd, 14.4, 10.0)	3.28 (dd, 14.0, 10.2)	3.39 (dd, 14.4, 8.0)	3.27 (dd, 14.4, 8.0)	3.35 (dd, 14.0, 10.8)	3.33 (s)	3.34 (dd, 13.3, 10.3)
9β	3.15 (dd, 14.4, 2.8)	3.29 (d, 14.4)	3.17 (d, 14.0)	3.28 (dd, 14.4, 3.2)	3.24 (m)	3.12 (d, 14.0)	3.33 (d, 11.0)	3.22 (d, 13.3)
13a			2.81 (ddd, 17.6, 6.5, 4.0)	2.89 (dt, 17.2, 5.2)	4.14 (2H, s)	4.39 (2H, s)		
13b			2.74 (ddd, 17.6, 6.5, 4.0)	2.66 (dt, 17.2, 5.2)				
14a	5.61 (s)		3.88 (ddd, 11.0, 6.5, 4.0)	3.82 (2H, t, 5.2)	5.05 (s)			
14b	6.19 (s)		3.86 (ddd, 11.0, 6.5, 4.0)		4.94 (s)			
15	2.48 (s)	2.47 (s)	2.49 (s)	2.46 (s)	2.50 (s)	2.51 (s)	2.49 (s)	2.50 (s)
16	1.33 (d, 7.2)	1.33 (d, 7.2)	1.35 (d, 7.6)	1.36 (d, 7.2)	1.37 (d, 7.2)	1.37 (d, 7.2)	1.35 (d, 7.2)	1.34 (d, 7.1)
OMe	3.76 (s)	3.65 (s)						

Table 2. ^{13}C-NMR Data (δ_C) of **1**—**8** in $CDCl_3$

No.	**1**	**2**	**3**	**4**	**5**	**6**	**7**	**8**
2	154.6	154.9	154.5	154.6	154.5	154.2	154.6	154.7
3	121.1	121.3	121.5	121.5	121.1	121.5	121.5	121.3
4	136.7	136.2	133.1	135.2	135.4	132.6	134.2	132.9
5	37.9	37.7	35	36.7	36.9	34.8	36.4	35.3
6	34	32.3	34.9	32.4	33.2	34.8	30.4	33.5
7	31.7	29.8	32.6	28.6	31.6	33.3	36.4	39.2
8	38	42.2	49.4	48.7	40	45.2	66.9	68.6
9	43.7	40.8	38.8	38.4	42.4	39.5	46.1	48.4
10	158.5	157.5	158.9	157.2	158.7	159.3	156.2	156.6
11	137.6	137.8	138.1	138	137.5	137.7	138.5	138.5
12	146.2	175.9	214	213.9	153.8	208.9		
13	167.5		43.2	43.8	65.1	66.8		
14	123.2		58.2	58.3	110.1			
15	23.9	24	23.6	23.6	23.8	23.6	23.8	23.9
16	18.3	18.9	20.5	19.1	18.8	20.4	19.7	20.1
OMe	51.9	51.7						

cycloheptane fused to the pyridine ring at C-10 and C-11. The correlations of H_3-OMe to C-13, and H_2-14 to C-8, C-12, and C-13 unequivocally established that the position of an isopropenoic acid methyl ester group was allowed to C-8.

The relative configuration of **1** was established by nuclear Overhauser effect spectroscopy (NOESY) correlations as shown in computer-generated 3D drawing (Fig. 2). The ^{3}J proton coupling constant ($^{3}J_{H\text{-}9\alpha/H\text{-}8}$=10.0 Hz) as well as NOESY correlations of H-9α/H_3-16 and H-9β/H-8 indicated that each of C-12 and C-16 adopted an α-configuration as shown in Fig. 2. Thus, the structure of **1** was established to be shown.

Rupestine G (**2**) gave a molecular formula of $C_{14}H_{19}NO_2$ as determined by the HR-ESI-MS at m/z 234.1509 $(M+H)^+$. IR absorptions implied the presence of carbonyl (1736 cm^{-1}) functionality. ^{1}H- and ^{13}C-NMR data (Tables 1, 2) revealed 14

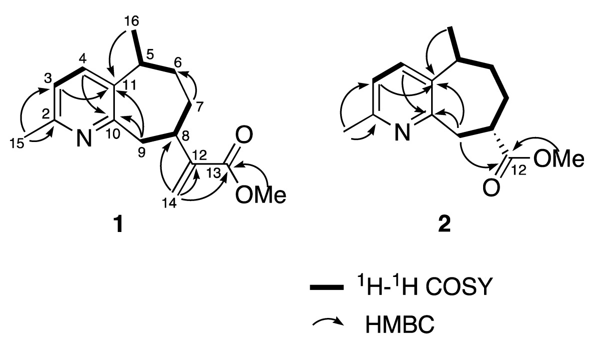

Fig. 1. Selected ^{1}H–^{1}H COSY and HMBC Correlations for Rupestines F—G (**1**—**2**)

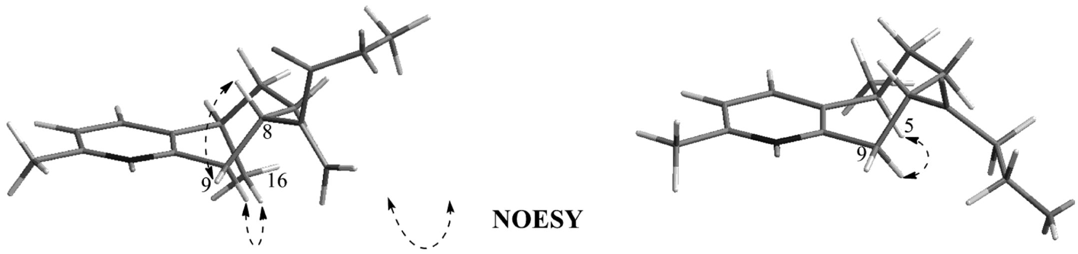

1 **3**

Fig. 2. Selected NOESY Correlations for Rupestines F (**1**) and H (**3**)

carbon signals due to three sp^2 quaternary carbons, two sp^2 methines, two sp^3 methines, three sp^3 methylenes, and three methyls (including one methoxy). Among them, three sp^2 quaternary carbons (δ_C 154.9, 157.5, 137.8) and two sp^2 methines (δ_C 121.3, 136.2) revealed the presence of a trisubstituted pyridine ring. The ^{1}H- and ^{13}C-NMR spectrum of **2** were quite similar to those of **1**, which suggested that **2** also possessed a guaipyridine sesquiterpene skeleton.

The connectivities of C-16 to C-9 were confirmed by ^{1}H ^{1}H COSY spectrum (Fig. 1). The HMBC correlations of H-9 to C-10 and C-11, and H_3-16 to C-11 gave rise to the connectivity of cycloheptene and pyridine rings through C-10 and C-11. The methoxy carbonyl side chain was deduced from the HMBC correlations of H-9 and H_3-OMe to C-12. Based on the NOESY correlations between H-9α and H_3-16, and the ^3J proton coupling constant ($^3J_{\text{H-9}\alpha/\text{H-8}}$=10.0 Hz), the relative configuration of C-5 and C-8 of **2** was concluded to be the same as **1**.

Rupestine H (**3**) had the composition of $C_{15}H_{21}NO_2$ by HR-ESI-MS [*m/z* 248.1665 $(M+H)^+$]. The ^{13}C-NMR data of **3** were analogous to those of **1** except for the substituent at C-8, and the ^{13}C resonances of one carbonyl (C-12, δ_C 214.0) and two sp^3 methylenes (C-13, δ_C 43.2; C-14, δ_C 58.2) were additionally observed in **3**. Based on the 2D-NMR data, the side chain of C-8 was deduced to be a 3-hydroxypropan-1-one moiety. The relative configuration of **3** was determined by a key rotating frame Overhauser enhancement spectroscopy (ROESY) (Fig. 2) correlation of H-5α/H-9α and the ^3J proton coupling constant ($^3J_{\text{H-9}\alpha/\text{H-8}}$=10.2 Hz) which revealed that C-16 was β-oriented and C-12 was α-oriented.

Rupestine I (**4**) possessed a molecular formula, $C_{15}H_{21}NO_2$ determined by HR-ESI-MS [*m/z* 248.1668 $(M+H)^+$]. ^{1}H- and ^{13}C-NMR data (Tables 1, 2) of **4** were similar to those of **3**, implying the isomeric nature for **3** and **4**. **4** was assumed to be an epimer of **3**, which was confirmed by the NOESY correlation between H-9α and H_3-16.

Rupestine J (**5**) had a molecular formula, $C_{15}H_{21}NO$ determined by the HR-ESI-MS [*m/z* 232.1724 $(M+H)^+$]. ^{1}H- and ^{13}C-NMR data (Tables 1, 2) of **5** revealed an *exo*-methylene group (δ_H 5.05, 4.94, δ_C 110.1). Based on the 2D-NMR data, the structure of **5** was assigned to be similar to **1**. The major difference was the presense of a hydroxy methyl (δ_C 65.1) at C-12 in **5** instead of a methoxycarbonyl group in **1**. Relative configuration of C-12 and C-16 was confirmed to be *cis*, since the NOESY correlation of H-9α/H_3-16 was observed.

Rupestine K (**6**) was assigned the molecular formula $C_{16}H_{19}NO_2$ through an analysis of its HR-ESI-MS [*m/z* 234.1517 $(M+H)^+$]. The NMR spectra (Tables 1, 2) of **6** closely matched with those of **3**. A significant difference was the presence of a hydroxy methyl at δ_C 66.8 connected to C-12 in **6** instead of a hydroxy ethyl in **3**. NOESY correlation of H-5α/H-9α and the ^3J proton coupling constant ($^3J_{\text{H-9}\alpha/\text{H-8}}$=10.8 Hz) suggested that the relative configurations of C-5 and C-8 in **6** were identical to those of **3**.

The molecular formula of rupestines L (**7**) and M (**8**) obtained as a pair of epimer, was determined to be $C_{12}H_{17}NO$ by analysis of the HR-ESI-MS and the NMR spectra (Tables 1, 2). Comparison of the NMR data of **1** and **8** indicated that the isopropenoic acid methyl ester group at C-8 in **1** was replaced by a hydroxy group in **8**, which was confirmed by COSY and HMBC experiments. Configuration of C-16 in **8** was found to be β-oriented on the basis of a ROESY cross-peak of H-5α/H-9α and the ^3J proton coupling constant ($^3J_{\text{H-9}\alpha/\text{H-8}}$=10.3 Hz). On the other hand, C-16 in **7** was assigned to be α-oriented, because ROESY correlations of H-9α/H_3-16 and H-9β/H-8 were observed.

The AC of **1**—**8** was assigned by using circular dichroism (CD) spectroscopy and time dependent density functional theory (TDDFT) calculations at B3LYP/TZVPP level. The CD spectra of **2**—**8** (see Experimental) showed a similar CD pattern, *i.e.* a negative Cotton effect (CE) near 270 nm and a positive CE in the 210—225 nm region, whereas some compounds exhibited a positive CE around 285 nm which may be attributed to the carbonyl group. The CE near 270 nm can be attributed to the pyridine ring, and thus the sign of this CE may be governed by the AC of C-5, by the preferred conformation, or by both the AC of C-5 and the preferred conformation. In contrast, the CD spectrum of **1** showed a different CD pattern, a negative CE at 213 nm and weak positive CEs above 220 nm. The difference may probably be caused by the additional α, β unsaturated ketone chromophore in **1**.

To study the effect of conformation to the CE sign at 270 nm, for possible conformations of model compounds 2-methylpyridinecycloheptene (**9**), **7** and **8**, their corresponding CD spectra were calculated (Figs. 3, 4). The calculation results are summarized as follow, (1) B3LYP/TZVPP calculations overestimated the excitation energy of pyridine's first absorption band (calc. *ca.* 250 nm *vs.* expt. *ca.* 270 nm), thus, the calculated CE around 250 nm will be observed experimentally around *ca.* 270 nm; (2) if the plane of C-6, C-7, and C-8 was above the pyridine ring, a positive CE around 215 nm and a negative CE around 250 nm are observed regardless of the chirality of C-5. Thus, using the CE sign around 270 nm, the absolute structure taken by the molecule can be deduced and the AC of C-5 and C-8 may be assigned accordingly.

Based on this conclusion, the AC of **2**—**8** was then assigned. According to the larger coupling between H-9α and

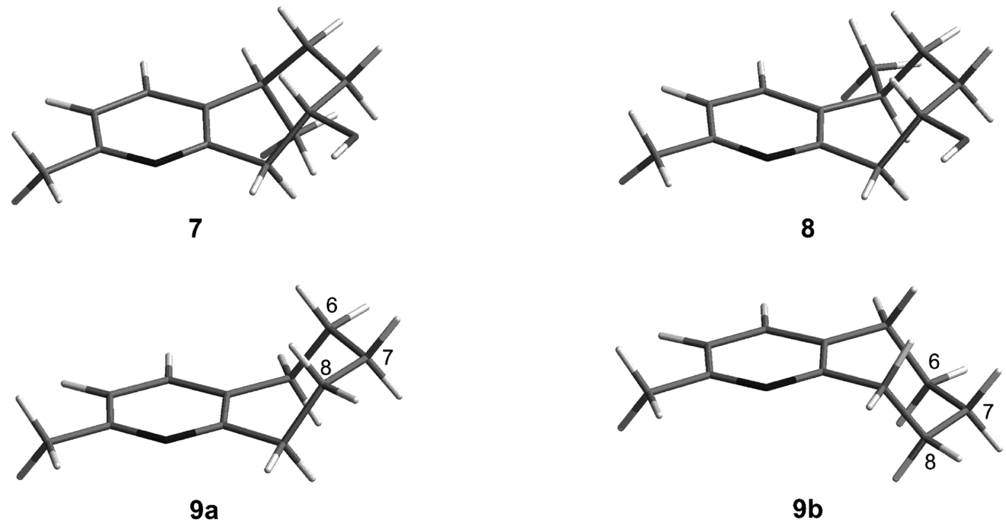

Fig. 3. Calculated Conformations of Model Compounds

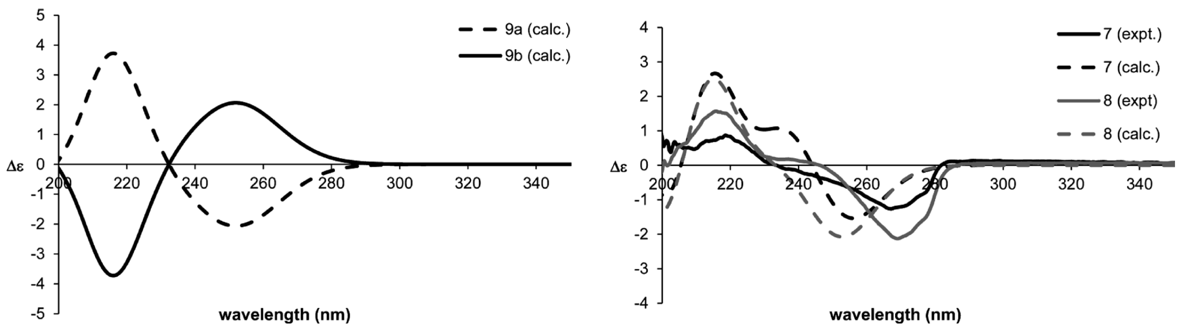

Fig. 4. Calculated CD Spectra of Model Compounds Together with the Experimental CD Spectra of **7** and **8**

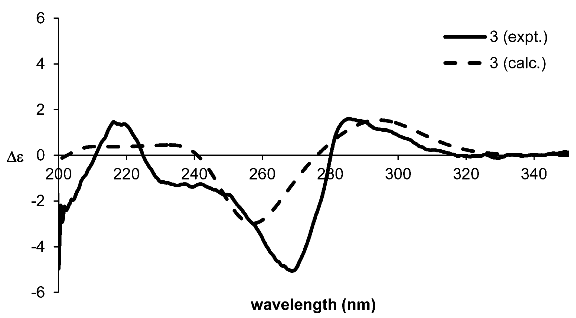

Fig. 5. Experimental CD Spectrum of **3** and Calculated CD Spectrum of the (5*S*,8*S*) of **3**

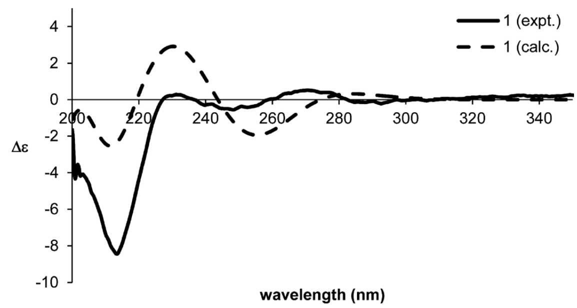

Fig. 6. Experimental CD Spectrum of **1** and Calculated CD Spectrum of the (5*S*,8*S*) of **1**

H-8 (Tables 1, 2) and conformational analysis by molecular mechanics calculation, **2**—**8** existed mainly in the chair conformation with the substituent at C-8 in the equatorial position. Experimental CD spectra of **2**—**8** implied the position of C-6, C-7, and C-8 to be above the pyridine ring, thus the configuration of C-8 should be *S* for **2** – **8**.

It has been mentioned that some compounds with a ketone group at C-12 exhibited a positive CE around 285 nm (**2**—**4**, **6**). Among these compounds, **3** was chosen as a representative and its AC was assigned by comparing the calculated CD spectra to the experimental one (Fig. 5).

The AC of **1**, which has a different CD pattern, was assigned by comparing the calculated CD spectra to the experimental one (Fig. 6). The calculated CD spectrum of the (5*S*,8*S*) isomer is similar to the experimental one, thus the AC of **1** was assigned as (5*S*,8*S*).

Experimental

General Experimental Procedures The UV spectra were obtained with a Ultrospec 2100 pro spectrophotometer. Optical rotations were measured with a JASCO DIP-1000 automatic digital polarimeter, and CD spectra were measured on a JASCO J-820 spectropolarimeter. IR spectra were recorded on a JASCO FT/IR–4100 spectrophotometer. High-resolution ESI-MS were obtained on a LTQ Orbitrap XL (Thermo Scientific). ^{1}H- and ^{13}C-NMR spectra were recorded on a

JEOL ECA600 spectrometer and a Bruker AV 400 spectrometer, and chemical shifts are referenced to the residual solvent peaks (δ_H 3.31 and δ_C 49.0 for methanol-d_4 and δ_H 7.26 and δ_C 77.0 for $CDCl_3$). Standard pulse sequences were employed for the 2D-NMR experiments.

Material The plant material of *A. rupestris* L. were collected from Hami City, Xinjiang Province, P.R. China, in June 2008, and was authenticated by Prof. Shi-Ming Duan (Xinjiang Institute of Ecology and Geography, Chinese Academy of Sciences). A voucher specimen has been deposited with Xinjiang Technical Institute of Physics and Chemistry, Chinese Academy of Sciences, P.R. China.

Extraction and Isolation The air dried and milled leaves of *A. rupestris* L. (10 kg) were extracted by maceration with MeOH (4×60 L, each time 2 d) at r.t. After filtration and evaporation of solvent under reduced pressure, the combined methanol extract (2.29 kg) was partitioned between 3% tartaric acid and $CHCl_3$ to obtain a water soluble fraction. The water soluble fraction was adjusted to pH 10 by saturated Na_2CO_3, then partitioned with $CHCl_3$ and *n*-BuOH, successively, to give $CHCl_3$ and *n*-BuOH fractions.

The $CHCl_3$ extract was chromatographed over CC (SiO_2; hexane/EtOAc, 8:1→2:1, and $CHCl_3$/MeOH 30:1→0:1) to afford 32 fractions. Fr. 4 was chromatographed over Sephadex LH-20 eluting with MeOH, then subjected to purification by preparative HPLC (C_{18}, MeOH/0.1% HCOOH aq., 2:3) to afford rupestine F (**1**, 4.7 mg). Fr. 9 was purified by preparative HPLC (C_{18}, MeOH/0.1% HCOOH aq., 3:7) to yield rupestine G (**2**, 0.5 mg). Fr. 15 was subjected to Sephadex LH-20 column (MeOH) to give 4 fractions, then the second fraction was subjected over a SiO_2 column (hexane/EtOAc 1:1, and then $CHCl_3$/MeOH 20:1→1:1) to afford 8 subfractions.

Sub. Fr. 7 was purified with C_{18} column (MeOH/0.1% HCOOH aq., 35:65) followed by preparative HPLC (C_{18}, MeOH/0.1% HCOOH aq., 18:82) to give rupestines H (**3**, 0.8 mg) and I (**4**, 1.9 mg). Sub. Fr. 4 was treated on amino silica gel (hexane/EtOAc, 1:1) and then purified by preparative HPLC (C_{18}, MeOH/0.1% HCOOH aq., 22:78 and MeOH/0.1% HCOOH aq., 14:86) to afford rupestines J (**5**, 0.7 mg), K (**6**, 0.9 mg), L (**7**, 0.8 mg), and M (**8**, 0.5 mg).

The *n*-BuOH fraction was separated over Sephadex LH-20 column chromatography (MeOH) to afford 4 fractions. Fr. 3 was further purified by an ODS column (40% MeOH) to give a known alkaloid, rupestine[4] (39.3 mg).

Rupestine F (**1**): Light yellow oil; $[\alpha]_D^{20}$ −62 (c=0.2, MeOH); UV λ_{max} (MeOH) nm (ε): 270 (3595) nm; CD λ_{max} (MeOH) nm ($\Delta\varepsilon$): 271 (+1.3), 246 (−0.5), 213 (−8.1); IR ν_{max} (CCl_4) cm^{-1}: 3057, 2952, 2927, 2852, 1723, 1626, 1591, 1573, 1461; ^1H- and ^{13}C-NMR data (Tables 1, 2); ESI-MS m/z 260 $[M+H]^+$; HR-ESI-MS m/z 260.1671 $[M+H]^+$ (Calcd for $C_{16}H_{22}NO_2$, 260.1651).

Rupestine G (**2**): Light yellow oil; $[\alpha]_D^{20}$ −16 (c=0.03, MeOH); UV λ_{max} (MeOH) nm (ε: 270 (3760), 213 (5644); CD λ_{max} (MeOH) nm ($\Delta\varepsilon$): 285 (0.06) 268 (−1.2), 224 (+0.4); IR ν_{max} (CCl_4) cm^{-1}: 2960, 2926, 2855, 1736, 1593, 1463; ^1H- and ^{13}C-NMR data (Tables 1, 2); ESI-MS m/z 234 $[M+H]^+$; HR-ESI-MS m/z 234.1509 $[M+H]^+$ (Calcd for $C_{14}H_{20}NO_2$, 234.1519).

Rupestine H (**3**): Light yellow oil; $[\alpha]_D^{20}$ +18 (c=0.1, MeOH); UV λ_{max} (MeOH) nm (ε): 270 (3939), 215 (5733) nm; CD λ_{max} (MeOH) nm ($\Delta\varepsilon$): 284 (+1.5), 268 (−5.0), 216 (+1.4); IR ν_{max} (CCl_4) cm^{-1}: 2959, 2925, 2854, 1707, 1463; ^1H- and ^{13}C-NMR data (Tables 1, 2); ESI-MS m/z 248 $[M+H]^+$; HR-ESI-MS m/z 248.1665 $[M+H]^+$ (Calcd for $C_{15}H_{22}NO_2$, 248.1651).

Rupestine I (**4**): Light yellow oil; $[\alpha]_D^{20}$ −12 (c=0.1, MeOH); UV λ_{max} (MeOH) nm (ε): 270 (3997) nm; CD λ_{max} (MeOH) nm ($\Delta\varepsilon$): 285 (+0.4), 267 (−6.9), 218 (−1.0); IR ν_{max} (CCl_4) cm^{-1}: 2958, 2926, 2855, 1708, 1951, 1462; ^1H- and ^{13}C-NMR data (Tables 1, 2); ESI-MS m/z 248 $[M+H]^+$; HR-ESI-MS m/z 248.1668 $[M+H]^+$ (Calcd for $C_{15}H_{22}NO_2$, 248.1651).

Rupestine J (**5**): Light yellow oil; $[\alpha]_D^{20}$ −17 (c=0.1, MeOH); UV λ_{max} (MeOH) nm (ε): 271 (3989), 215 (6545) nm; CD λ_{max} (MeOH) nm ($\Delta\varepsilon$): 270 (−5.1), 224 (+0.1); IR ν_{max} (CCl_4) cm^{-1}: 2951, 2926, 2855, 1590, 1463; ^1H- and ^{13}C-NMR data (Tables 1, 2); ESI-MS m/z 232 $[M+H]^+$; HR-ESI-MS m/z 232.1724 $[M+H]^+$ (Calcd for $C_{15}H_{22}NO$, 232.1701).

Rupestine K (**6**): Light yellow oil; $[\alpha]_D^{20}$ +20 (c=0.03, MeOH); UV λ_{max} (MeOH) nm (ε): 271 (3712), 215 (5483) nm; CD λ_{max} (MeOH) nm ($\Delta\varepsilon$): 282 (+2.2), 267 (−4.8), 217 (+2.0); IR ν_{max} (CCl_4) cm^{-1}: 2958, 2925, 2855, 1710, 1591, 1463; ^1H- and ^{13}C-NMR data (Tables 1, 2); ESI-MS m/z 234 $[M+H]^+$; HR-ESI-MS m/z 234.1517 $[M+H]^+$ (Calcd for $C_{16}H_{20}NO_2$, 234.1494).

Rupestine L (**7**): Light yellow oil; $[\alpha]_D^{20}$ −40 (c=0.03, MeOH); UV λ_{max} (MeOH) nm (ε): 270 (4026), 215 (5630) nm; CD λ_{max} (MeOH) nm ($\Delta\varepsilon$): 267 (−1.3), 218 (+0.9); IR (CCl_4) ν_{max} 2960, 2926, 2856, 1590, and 1464 cm^{-1}; ^1H- and ^{13}C-NMR data (Tables 1, 2); ESI-MS m/z 192 $[M+H]^+$; HR-ESI-MS m/z 192.1384 $[M+H]^+$ (Calcd for $C_{12}H_{18}NO$, 192.1388).

Rupestine M (**8**): Light yellow oil; $[\alpha]_D^{20}$ −38 (c=0.05, MeOH); UV λ_{max} (MeOH) nm (ε): 270 (3900), 215 (5052) nm; CD λ_{max} (MeOH) nm ($\Delta\varepsilon$): 267 (−3.0), 215 (+2.3); IR (CCl_4) ν_{max} 2961, 2925, 2856, and 1462 cm^{-1}; ^1H- and ^{13}C-NMR data (Tables 1, 2); ESI-MS m/z 192 $[M+H]^+$; HR-ESI-MS m/z 192.1378 $[M+H]^+$ (Calcd for $C_{12}H_{18}NO$, 192.1388).

Computational Details The CD calculations performed by Turbomole 6.3[8] using TD-DFT-B3LYP/TZVPP level of theory on RI-DFT-B3LYP/TZVPP optimized geometries.[9—15] The conformer used for CD calculation was the model obtained by using MC calculations (MMFF94 force field,[16] Macromodel 9.1).[17] The CD spectra were simulated by overlapping Gaussian functions for each transition where the width of the band at 1/e height is fixed at 0.3 eV or 0.25 eV, and the resulting spectra were scaled to the experimental values.

Acknowledgments This work was partly supported by the National Science Foundation of China (No. 20872174), the CAS/SAFEA International Partnership Program for Creative Research Teams and the High-Tech Research and Development Program of Xinjiang (No. 200910105), a Grant-in-Aid for Scientific Research from the Ministry of Education, Culture, Sports, Science and Technology of Japan, and a Grant from the Open Research Center Project.

References and Notes

1) Liu Y. M., "Pharmacography of Uighur," Xinjiang People's Publishing House, Urumqi, 1986.
2) Chen X. Y., Wang S. H., *J. Chin. Tradit. Herb. Drugs*, **12**, 25 (1981).
3) Yong J. P., Aisa H. A., Nie L. F., *Chin. J. Chem. Sep. Sci.*, **29**, 1640—1644 (2009).
4) Su Z., Wu H. K., Yang Y., Aisa H. A., Slukhan U., Aripova S., *J. Sep. Sci.*, **31**, 2161—2166 (2008).
5) Su Z., Wu H. K., He F., Slukhan U., Aisa H. A., *Helv. Chim. Acta*,

93, 33—38 (2010).
6) Hsieh T. J., Chang F. R., Chia Y. C., Chen C. Y., Chiu H. F., Wu Y. C., *J. Nat. Prod.*, **64**, 616—619 (2001).
7) Büchi G., Goldman I. M., Mayo D. W., *J. Am. Chem. Soc.*, **88**, 3109—3113 (1966).
8) "TURBOMOLE V6, 3, 2011, a Development of University of Karlsruhe and Forschungszentrum Karlsruhe GmbH, 1989—2007, TURBOMOLE GmbH, since 2007.": ‹http://www.turbomole.com›.
9) Eickorn K., Treutler O., Ohm H., Haser M., Ahlrichs R., *Chem. Phys. Lett.*, **240**, 283—289 (1995).
10) Becke A. D., *Phys. Rev. A*, **38**, 3098—3100 (1988).
11) Lee C., Yang W., Parr R. G., *Phys. Rev. B*, **37**, 785—789 (1988).
12) Halgren T. A., *J. Am. Chem. Soc.*, **112**, 4710—4723 (1990).
13) Halgren T. A., *J. Am. Chem. Soc.*, **114**, 7827—7843 (1992).
14) Halgren T. A., *J. Comput. Chem.*, **17**, 490—519 (1996).
15) Halgren T. A., *J. Comput. Chem.*, **17**, 520—552 (1996).
16) Schafer A., Horn H., Ahlrichs R., *J. Chem. Phys.*, **100**, 5829—5835 (1994).
17) Mohamadi F., Richards N. G. J., Guida W. C., Liskamp R., Lipton M., Caufield C., Chang G., Hendrickson T., Still W. C., *J. Comput. Chem.*, **11**, 440—467 (1990).